Controlling growth and morphogenesis of the industrial enzyme producer Streptomyces lividans

Mangiameli, G.

Chapter 4

Analysis of the transcriptome of *Streptomyces lividans cslA* and *glxA* null mutants reveals disturbance in the transcription of genes relating to morphogenesis and osmoprotection

Giulia Mangiameli, Erik Vijgenboom, Dennis Claessen and Gilles P. van Wezel

ABSTRACT

Streptomyces mutants lacking genes *cslA* and *glxA* grow as an open mycelium in liquid cultures. Such a non-pelleting phenotype may be of interest from the perspective of industrial applications. *cslA* and *glxA* form an operon, whereby *cslA* encodes a cellulose synthase-like protein, while *glxA* encodes a copper oxidase. Both proteins are involved in the synthesis and deposition of a glycan at hyphal tips. The absence of this polysaccharide is linked to an alteration in the formation of the matrix and in the aggregation of pellets. To better understand which changes are induced in the mutants and to identify potential targets for the control of morphology, global transcriptome profiling was performed taking advantage of the last generation RNA sequencing (RNA-Seq) with Illumina technology. This led to the identification of genes that are potentially involved in morphogenesis and matrix formation, including a cluster that encodes phage tail-related proteins. The increased expression of genes related to osmoprotection indicates that, in addition, the mutants suffer from osmotic stress. Taken together, the data provide interesting new insights into the role of CslA and GlxA in the control of morphogenesis and stress management.

INTRODUCTION

Streptomycetes are mycelial soil bacteria that grow as an intricate network of branched hyphae. After vegetative growth, the colonies develop and produce aerial hyphae, which grow in the air and eventually differentiate to generate chains of spores. The formation of aerial hyphae is facilitated by various macromolecules. The lantibiotic-like peptide SapB is involved in lowering the water surface tension at the medium-air interface (Willey et al. 1991; Willey et al. 1993), which enables hyphae to leave the aqueous environment. Aerial hyphae then become decorated with a mosaic of pair-wise aligned fibrils, which is known as the rodlet layer. Formation of this surface layer requires the activity of two types of proteins, called chaplins and rodlins. Chaplins are the main constituents of the rodlet layer and were shown to assemble into small fibrils. *In vivo*, these fibrils are deposited in an often pair-wise aligned arrangement on the cell surface by the activity of the rodlins.

Recent evidences unambiguously demonstrated that the chaplins assemble into so-called amyloid structures (Sawyer et al. 2011; Bokhove et al. 2013). Amyloids are proteinaceous aggregates that are rich in β-sheet structure. Amyloid fibrils are associated with the surfaces of many bacteria and fungi, often having roles in biofilm formation, but also in providing surface hydrophobicity or protection. Examples are curli fibers in *E. coli* (Zogaj et al. 2003) and thin aggregative fimbriae (tafi) in *Salmonella* species (White et al. 2003), which are involved in biofilm formation, and hydrophobins of filamentous fungi, which render the aerial hyphae hydrophobic in a similar manner as chaplins do for streptomycetes (Wösten et al. 1999; Linder et al. 2005) .

In addition to their role in aerial growth, the *Streptomyces* chaplin proteins are involved in attachment of hyphae to surfaces. Attachment coincides with the formation of a so-called extracellular matrix (de Jong et al. 2009). This matrix is composed of assembled chaplin amyloid fibrils in association with a polymer produced by a protein annotated as a cellulose synthase-like protein, CslA (Xu et al., 2008). The absence of CslA leads to an arrest of development on rich solid media (Xu *et* al, 2008)

and strongly decreases attachment (de Jong et al., 2009; Chapter 2). CslA is required for the synthesis of a β-(1,4) polymer, although the exact nature of the polymer is unclear. These results demonstrate the important roles that macromolecules play during growth and development of streptomycetes.

Although development is mostly associated with growth on solid substrates, *Streptomyces* also differentiate in liquid-grown cultures. Some streptomycetes fragment and sporulate in submerged cultures, such as the chloramphenicol producer *S. venezuelae* and the streptomycin producer *S. griseus*, whereby submerged sporulation correlates to the specific amino acid sequence (and expression level) of the SsgA and SsgB proteins (Girard et al. 2013), which control sporulation-specific cell division (Willemse et al. 2011). Many strains, however, form so-called pellets in liquid media (Pamboukian et al. 2002). Interestingly, deletion of genes encoding for cell surface proteins such as the chaplins or CslA strongly reduces the size and changes the morphology of pellets (van Veluw et al. 2012; Chapter 3). Recent data indicates that CslA acts in conjuction with GlxA, a copper oxidase with remote similarity to galactose oxidases (Liman et al. 2013), encoded by a gene adjacent to (and cotranscribed with) *cslA*. In particular, the *cslA* and *glxA* mutants form open mycelial structures when grown in rich liquid media (Fig. 1). This effect is likely explained by the absence of a glycan-like polysaccharide, synthesized at the hyphal tips by CslA and associated to the cell wall via non-covalent interactions after modification by GlxA. While the absence of CslA leads to a complete block in polymer formation, the absence of GlxA caused the CslA-produced polymer to be mislocalized. A role for the glycan in hyphal aggregation has therefore been postulated (Chapter 3).

The phenotypes associated with the changes in morphology in liquid-grown cultures will inevitably lead to changes in gene expression. To obtain more insight into the changes as a result of the deletion of *cslA* and *glxA*, global transcription profiling was performed using RNA-Seq analysis. The results not only demonstrate the impact of CslA and GlxA on *Streptomyces* physiology, but also point at genes that may play a role in the observed morphological changes in liquid-grown cultures.

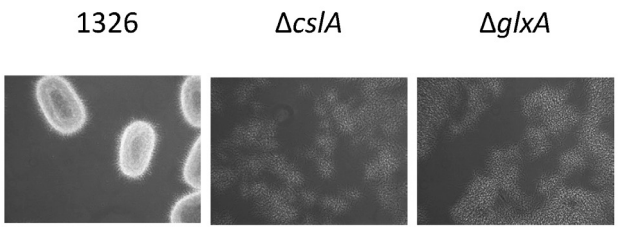

Figure 1. Phenotypic comparison between the wild-type (1326) and the corresponding Δ*cslA* and Δ*glxA* mutants in liquid-grown cultures

RESULTS AND DISCUSSION

Transcriptome analysis of the cslA *and* glxA *mutants*

The global transcription profiles of the *cslA* and *glxA* mutants were compared to those of the parental strain *S. lividans* 1326 and to one another, using RNA seq analysis. For this, RNA was isolated from liquid-grown cultures in the mid-exponential growth phase and sequenced as described in the Materials and Methods section. For the analysis of the transcriptome data, a change of two-fold or more in transcript levels and an RPKM value >10 were chosen as cut-off (RPKM: Reads per Kilobase of exon model per Million mapped reads; Mortazavi et al. 2008).

An overview of the number of genes whose transcription was changed according to the criteria set above is given in Figure 2, while the corresponding RPKM values and fold changes of those genes are provided in the Appendix.

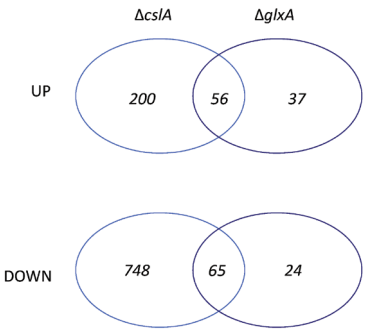

Figure 2. Venn diagram showing the number of genes uniquely up- or down regulated in the *cslA* and *glxA* mutant and those shared by the two mutants.

Following these criteria, deletion of *cslA* resulted in 256 genes whose transcription was upregulated and 813 genes whose transcription was downregulated in comparison to the parental strain. For the *glxA* mutant, 93 genes were upregulated and 89 genes downregulated. Most genes whose transcription levels were changed in the *glxA* mutant showed comparable changes in the *cslA* mutant (Fig. 2 and Appendix).

Despite the remarkable changes in the expression profile, few changes in the transcription of genes encoding transcriptional regulators were observed (Tables S1 and S2). Among the TetR regulators, which control among others efflux pumps and osmotic stress, five genes are upregulated in the *glxA* mutant (SLI_0468, SLI_0641, SLI_2006, SLI_3521 and SLI_4911). Two ArsR regulators (SLI_1107, SLI_7362), involved in modulating metal resistance and stress, are about two-fold upregulated in the *glxA* mutant, while SLI_1891 and SLI_5378, belonging to the GntR family that regulate general metabolism, are two-fold down in both *cslA*/*glxA* mutants.

Changes in transcription of genes related to pellet morphology

In the *cslA* null mutant, transcription of *glxA* was upregulated around 18-fold, perhaps as an attempt to compensate for the absence of the functionally linked *cslA*. Transcripts corresponding to the remainder of *cslA* were also enhanced in the *cslA* mutant (around 17-fold) (Table 1). Interestingly, such a strong increase in transcription of *cslA-glxA* was not observed in the *glxA* mutant. This suggests the presence of a CslA-dependent feedback mechanism that is involved in coordination of *glxA* and *cslA* transcription.

Transcription of SLI_3189, located directly next to the *cslA-glxA* gene cluster, is two-three fold enhanced in *glxA* and *cslA* mutants respectively (Table 1). It encodes a glycosyl hydrolase previously suggested to be functionally related to CslA and GlxA (Liman et al. 2013). However, our unpublished data suggest that the gene does not play a major role in the control of morphogenesis (D. Claessen, personal communication).

Previous work demonstrated that the overexpression of the *ssgA* gene (SLI_4184) leads to smaller pellets due to increased fragmentation (van Wezel et al. 2006). Furthermore, the deletion of *ssgA* causes a two- to six-fold increase in transcription of *glxA* (Noens et al. 2007). However, in our data no changes in the level of *ssgA* were observed in the *glxA* and *cslA* mutants as compared to the parental strain (Table 1). Pellet morphology is also influenced by the chaplin genes (de Jong et al. 2009; van Veluw et al. 2012; M.L.C. Petrus and D. Claessen, unpublished data). By looking at the transcription of the long chaplins (SLI_3063, SLI_7473, SLI_1979) and short chaplins (SLI_3064, SLI_2108, SLI_3053, SLI_3047, SLI_1980), substantial differences were observed only in the case of SLI_1980 (*chpH*), with a near two-fold increase in the *cslA* mutant, and SLI_7473 (*chpB*), with is around two-fold downregulated in both mutants (Table1).

Table 1. Expression analysis of genes known to be involved in pellet morphology

Gene # *S. coelicolor*	Gene # *S. lividans*	1326 (RPKM)	cslA (RPKM)	glxA (RPKM)	cslA/1326	glxA/1326	Annotation
SCO2836	SLI3187	136,3	167,3	129,4	1,2	0,9	CslA
SCO2837	SLI3188	188,4	3460,9	1,1	18,4	0,0	GlxA
SCO2838	SLI3189	172,9	529,4	312,0	3,1	1,8	glycosyl hydrolase
SCO3926	SLI4184	24,0	20,8	32,4	0,9	1,3	SsgA
SCO2716	SLI3063	1,1	1,6	1,1	1,4	1,0	ChpA
SCO7257	SLI7473	25,0	14,0	12,1	0,6	0,5	ChpB
SCO1674	SLI1979	32,6	32,0	24,7	1,0	0,8	ChpC
SCO2717	SLI3064	6,4	3,4	4,9	0,5	0,8	ChpD
SCO1800	SLI2108	100,6	147,6	69,9	1,5	0,7	ChpE
SCO2705	SLI3053	6,7	11,3	8,5	1,7	1,3	ChpF
SCO2699	SLI3047	2,5	5,3	3,8	2,2	1,5	ChpG
SCO1675	SLI1980	61,8	117,0	62,3	1,9	1,0	ChpH
SCO7657	SLI7885	532,7	985,9	809,2	1,9	1,5	HyaS

Other genes relating to morphology include SLI_7885, which encodes the hyphal aggregation protein HyaS. Transcription of *hyaS* was between 1.5- and 1.9-fold enhanced in the *glxA* and *cslA* mutants (Table 1). HyaS is a putative lysyl/amine oxidase with a suggested role in hyphal aggregation and pellet formation in liquid cultures. Its deletion decreases pellet density and leads to abundant protrusion of hyphae from the pellet surface (Koebsch et al. 2009). Increased transcription of the *hyaS* gene could indicate a compensation effect for the loss of pellet integrity.

Enhanced transcription of a cluster of genes for phage tail-related proteins

Analysis of the differentially transcribed genes indicated that transcription of the gene cluster SLI_4479-SLI_4495 was significantly enhanced in the *cslA* and *glxA* mutants, namely between 1.5-2.5 fold in the *glxA* mutant and between two to five-fold in the *cslA* mutant. These genes are organized in five sets of genes, four of which were suggested to be transcribed from two divergent promoters in *S. coelicolor* (Kim et al. 2005; Table 2 and Figure 3A). The presence of genes SLI_4479-4485 and SLI_4487-4489 is highly conserved among Actinomycetales. They may have been acquired via horizontal transfer, as suggested by the presence immediately upstream of SLI_4478 of a gene for the threonine tRNA that recognises ACA codons. tRNA genes often serve as sites for exogenous gene integration (Williams 2002).

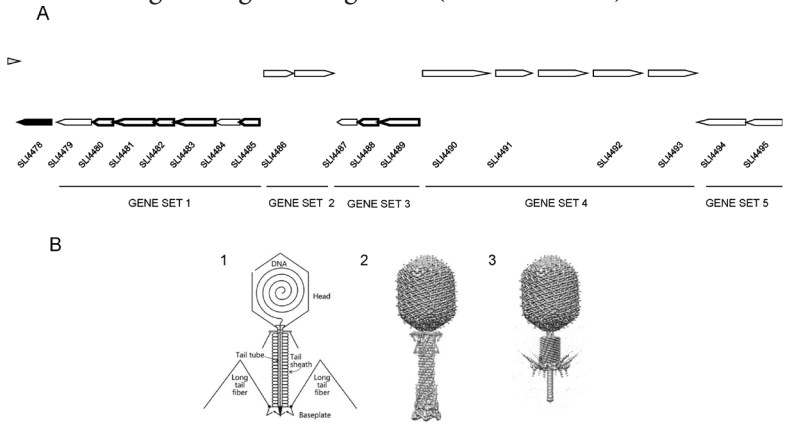

Figure 3. (A) The SLI4479-4495 cluster in *S. lividans*. Thick arrows indicate genes for phage assembly proteins, black arrows genes not involved in the cluster and triangle tRNA genes (B) A representation of phage proteins in the bacteriophage T4 (picture taken from Leiman et al. 2010) (1) Schematic representation of the assembly of the phage and conformation prior to (2) and during (3) bacterial infection.

Table 2. Upregulation of the cluster SLI4479-SLI4495. Two gaps were detected in the *S. lividans* genome sequence, corresponding to the *S. coelicolor* SCO4250 and SCO4256 genes. The data for these genes were obtained with the *S. coelicolor* genome as a reference and normalization of the RPKM values between the two data sets.

Gene # *S. coelicolor*	Gene # *S. lividans*	1326 (RPKM)	cslA (RPKM)	glxA (RPKM)	cslA/1326	glxA/1326	Annotation
SCO4243	SLI4480	24,9	98,3	60,7	3,9	2,4	secreted protein
SCO4244	SLI4481	39,3	146,7	85,3	3,7	2,2	hypothetical protein
SCO4245	SLI4482	40,4	146,1	87,9	3,6	2,2	hypothetical protein
SCO4246	SLI4483	38,4	165,0	93,3	4,3	2,4	hypothetical protein
SCO4247	SLI4484	56,0	249,4	138,1	4,5	2,5	hypothetical protein
SCO4248	SLI4485	37,2	174,2	94,9	4,7	2,5	hypothetical protein
SCO4249	SLI4486	18,2	57,5	30,0	3,2	1,7	hypothetical protein
SCO4250		116,7	299,3	128,0	2,6	1,1	ampullate spidroin
SCO4251	SLI4487	575,8	2311,7	1137,6	4,0	2,0	secreted protein
SCO4252	SLI4488	845,1	4425,2	2045,2	5,2	2,4	hypothetical protein
SCO4253	SLI4489	550,1	2388,0	1065,2	4,3	1,9	Phage tail sheath protein FI
SCO4254	SLI4490	12,2	25,2	20,0	2,1	1,6	Hypothetical protein
SCO4255	SLI4491	20,7	73,8	42,5	3,6	2,1	Conserved hypothetical protein
SCO4260		10,5	26,7	29,5	2,6	2,8	hypothetical protein
SCO4257	SLI4492	73,4	236,8	192,1	3,2	2,6	Hydrolytic protein
SCO4258	SLI4493	101,4	325,3	193,6	3,2	1,9	Hydrolytic protein
SCO4259	SLI4494	29,0	94,4	54,5	3,3	1,9	ATPase AAA
SCO4260	SLI4495	80,8	158,2	123,5	2,0	1,5	hypothetical protein

Interestingly, several of the proteins encoded within the gene cluster show striking similarities with those involved in phage assembly. Seven genes encode morphogenetic phage proteins (indicated with thick arrows in Fig. 3A), whose role in the assembly of phages has been recently reviewed (Leiman et al. 2010 and Fig 3B). SLI_4480-SLI_4481 and SLI_4488_SLI_4489 are annotated as genes encoding phage tail proteins. In bacteriophage T4, phage tail proteins organize in a contractile helical structure that is part of the phage tail. Contraction leads to penetration of the cell membrane by the central tail tube and injection of the DNA into the bacterial cell. The protein encoded by SLI_4485 shows similarities with the tail tube. Other phage-related proteins include those encoded by SLI_4483 and SLI_4482, which could form a baseplate component with acidic lysozyme activity, used by viruses to digest the peptidoglycan of the bacterial cell envelope and inject the DNA directly into the cytosol. SLI_4484 encodes a protein with a LysM domain. Proteins containing such domains are typically involved in binding to peptidoglycan and chitin in bacteria and eukaryotes, respectively (Buist et al. 2008). The transcript levels of SLI_4498, described in the past as the transcriptional regulator of at least three of the five gene sets in *S. coelicolor* (Kim et al. 2005), was not significantly changed in *cslA* and *glxA* mutants. This suggests that either the activation of the transcriptional activator is post-translationally regulated, or that its role at least under these conditions is limited.

Phage-related proteins are present in many bacteria, although knowledge about their biological significance is limited. In the pathogenic *E. coli* strain O157:H7, phage tail proteins are described as collagen-like proteins which may play a role in virulence (Ghosh et al. 2012). Similarly, collagen-like proteins have been described in *Streptococcus pyogenes*, with a role in cell adhesion and pathogenicity (Chen et al. 2010). In the food pathogen *Cronobacter sakazakii*, biofilm and extracellular matrix formation are affected in mutants lacking, among others, phage tail proteins (Du et al. 2012). It is interesting to notice that SLI_4488 is one of the most strongly expressed genes in terms of absolute RPKM, with transcription comparable to that of ribosomal protein genes, which suggests a pivotal role for the protein encoded by this gene.

In contrast to genes SLI_4479-4485 and SLI_4487-4489, the presence of

SLI_4486 is less well conserved. In *S. coelicolor*, the homologous SCO4249 is coupled to SCO4250, encoding a protein with weak similarity to the major ampullate spidroin of *Nephila madagascariensis* (Gatesy et al. 2001). In *S. lividans*, there is a gap in the genome sequence, but analysis of the transcription data using the *S. coelicolor* genome as reference suggests that the gene is present but not annotated (data not shown). Spidroin is the major constituent of spider-silk, whose final fiber has striking similarities with amyloid fibrils (Kenney et al. 2002). Amyloid fibrils have an important role in attachment and biofilm formation in various organisms (Zogaj et al. 2003; White et al. 2003; Linder et al. 2005) including *Streptomyces* (Claessen et al. 2003; de Jong et al. 2009; Gras and Claessen, 2014).

The putative role for phage tail proteins in biofilm formation may suggest a role for these proteins in the formation of an extracellular matrix in streptomycetes, perhaps in conjuncion with the glycan produced by CslA and GlxA and possibly the chaplins (M.L.C. Petrus and D. Claessen, unpublished data). Their increased transcription might reflect a compensation effect for the loss of pellet architecture. Notably, the involvement of this gene cluster in morphogenesis has been observed previously in a non-pelleting mutant of *S. lividans* (MD Dissel and GP van Wezel, unpublished data). If and how these proteins contribute to extracellular matrix formation and pellet aggregation in *Streptomyces* is under current investigation.

Transcription of genes related to osmoprotection

A second category of genes that stood out in terms of being significantly enhanced in the *cslA* and *glxA* mutants were those encoding ABC transporters for the uptake of amino acids. These include SLI_3177-3180, which lie adjacent to the *cslA-glxA* genes (Table S1). Interestingly, genes SLI_1923-1924 for the putative glycine transporter are also upregulated in the mutants, as well as SLI_5103-5105, which are part of an operon together with SLI_5101-5102, encoding a choline and an aldehyde dehydrogenase (Table 3). Glycine forms bridges in the peptidoglycan in Gram-positive bacteria (Leyh-Bouille et al. 1977). Moreover, glycine betaine is a cellular osmoprotectant that accumulates in the cytoplasm to provide protection against osmotic stress (Landfald

and Strøm 1986; Bursy et al. 2008). Glycine betaine can be imported in the cell via specific ABC transporters or synthesized from glycine (Kimura et al. 2010) or from precursors choline and glycine betaine aldehyde (Lamark et al. 1991). The two best studied systems are genes *betTIBA* in *E. coli* (Lamark et al. 1991) and genes *opuABC* and *gbsAB* in *B. subtilis* (Kappes et al. 1999).

In the *cslA* and *glxA* mutants, transcription of SLI_1923 (an OpuABC-like permease) and SLI_1924 (the likely ATPase of the uptake system) was six- and almost four-fold enhanced, respectively (Table 3). In addition, two- to five-fold upregulation is observed for genes SLI_5101 (similar to *B. subtilis* GbsAB dehydrogenases), SLI_5102, (a putative choline dehydrogenase), SLI_5103 (an ATP-binding protein), SLI_5104 (similar to *B. subtilis* OpuAB transporters) and SLI_5105 (a possible glycine betaine substrate binding protein).

Another molecule that accumulates in the cell in response to salt and temperature stress is ectoine (Bursy et al. 2008). Transcription of the genes involved in ectoine biosynthesis (SLI_2175-2178) was approximately two-fold increased in the *glxA* mutant and between three- and ten-fold in the *cslA* mutant (Table 3). Ectoine is a natural osmoprotectant that is either imported or synthesized through the conversion of the precursor, L-aspartate-β-semialdehyde, via four enzymatic steps involving: acetyl-transferase EctA (SLI_2175), aminotransferase EctB (SLI_2176), ectoine synthase EctC (SLI_2177) and hydroxylase EctD (SLI2178) (Bursy et al. 2008). The increased transcription of genes for choline/glycine betaine transporters and for ectoine synthesis may reflect increased osmotic stress in *glxA* and *cslA* mutants. We hypothesize that the glycan synthesized by CslA and GlxA may play an important role in osmoprotection; in that model, upregulation of genes for osmoprotectants (such as glycine betaine and ectoine) is an attempt to compensate for the absence of the glycan in *cslA* mutants, or of the mature glycan in *glxA* mutants.

Finally, strong downregulation was observed for SLI_3420-3423 and SLI_5205, all of which are involved in histidine catabolism (Table 3). This may reflect an attempt to maintain the histidine pool during osmotic stress. Histidine is a precursor of ergothioneine, a thiourea derivative that is synthesized via methylation of histidine

and incorporation of a cysteine-derived sulfur atom in the imidazole ring (Seebeck 2013). Ergothioneine, naturally produced by Actinobacteria and by filamentous fungi, acts as an efficient antioxidant (Cheah and Halliwell 2012). A possible role of histidine/ergothioneine accumulation in osmotic stress in *Streptomyces* should be investigated.

However, changes in the transcription of known osmotic stress regulatory genes such as *sigB* and *osaC* were not observed, with only a partial effect on *osaB* in the *cslA* mutant (Fernández Martínez et al. 2009 and Table 5). This is consistent with earlier work, where the regulation of *glxA* by these elements has been ruled out (Liman et al. 2013).

CONCLUSION

The analysis of the transcriptome of the mutants reveals a large number of genes whose transcription is significantly up- or downregulated. The most drastic changes are observed in *cslA* mutants. Two classes of genes stood out, namely genes for phage tail-like proteins that possibly relate to matrix formation/morphology and genes related to osmoprotection. Phage tail-like proteins (SLI_4479-4495) are upregulated three to five-fold in the *cslA* mutant and around two-fold in the *glxA* mutant. Their role in bacteria is not clear, but their function in attachment to the bacterial cell wall and their role in biofilm formation suggests a structural role. Moreover, a change in transcription has been observed in other strains with a nonpelleting phenotype, suggesting a direct correlation with pellet morphology. In addition *hyaS*, involved in hyphal aggregation, is also upregulated in both mutants, suggesting that a network of proteins might interact in the determination of morphology. We currently favor a model in which the absence of one of them leads to a compensation effect increasing the transcription of the others. However, this awaits further experimental evidence.

In addition to the observed effect on morphology-related genes, deletion of *cslA* and *glxA* also majorly influence the transcription of genes related to osmoprotection.

Table 3. Transcription data of genes linked to osmotic stress

Gene # *S. coelicolor*	Gene # *S. lividans*	1326 (RPKM)	cslA (RPKM)	glxA (RPKM)	cslA/1326	glxA/1326	Annotation
SCO1620	SLI1923	31,5	193,9	117,3	6,2	3,7	Glycine betaine ABC transport system
SCO1621	SLI1924	28,7	153,3	106,7	5,3	3,7	L-proline glycine betaine ABC transport system
SCO4828	SLI5101	20,9	49,8	48,8	2,4	2,3	Betaine aldehyde dehydrogenase GsbAB (EC 1.2.1.8)
SCO4829	SLI5102	17,8	62,4	48,6	3,5	2,7	Choline dehydrogenase (EC 1.1.99.1)
SCO4830	SLI5103	8,2	41,1	26,2	5,0	3,2	Glycine betaine ABC transport system, ATP-binding protein (EC 3.6.3.32)
SCO4831	SLI5104	8,1	33,2	22,0	4,1	2,7	Glycine betaine ABC transport system, permease protein OpuAB
SCO4832	SLI5105	24,4	67,4	50,1	2,8	2,1	Choline/glycine betaine ABC transporter, substrate binding protein
SCO1864	SLI2175	32,4	94,2	52,1	2,9	1,6	L-2,4-diaminobutyric acid acetyltransferase (EC 2.3.1.-)
SCO1865	SLI2176	31,3	167,0	61,8	5,3	2,0	Diaminobutyrate-pyruvate aminotransferase (EC 2.6.1.46)
SCO1866	SLI2177	67,7	666,0	139,3	9,8	2,1	L-ectoine synthase (EC 4.2.1.-)
SCO1867	SLI2178	72,5	614,8	125,1	8,5	1,7	Ectoine hydroxylase (EC 1.17.-.-)
SCO0600	SLI0566	33,1	36,2	35,9	1,1	1,1	sigma factor SigB
SCO5749	SLI6010	447,5	262,7	342,2	0,6	0,8	OsaB
SCO5747	SLI6008	63,7	43,6	56,9	0,7	0,9	OsaC

In the *cslA* and *glxA* mutants, we observed an increase in transcription of genes related to ectoine synthesis and glycine betaine import and synthesis. We postulate that the absence of the polymer synthesized and deposited at the hyphal tips by the concerted action of *cslA* and *glxA* induces possible weakness to the hyphae, which stimulates the increase of intracellular osmoprotectants. The fact that the deletion of *cslA* almost invariably results in stronger changes in gene expression than deletion of *glxA* may be explained by the absence of the glycan in the *cslA* mutant, while this polysaccharide is present but not localized properly in the *glxA* mutant.

Future work is aimed at further analysis and verification of the major changes observed by RNA seq analysis, and to study the role of the phage tail proteins in the control of morphogenesis. In this way we will obtain more insight into the factors that play a role in controlling mycelial architecture.

MATERIAL AND METHODS

Strains and growth conditions

Streptomyces lividans strains 1326 (*S. lividans* 66, stock number 1326 from the John Innes Centre; Hopwood et al. 1985), and the Δ*cslA* and Δ*glxA* derivatives thereof (Chapter 3) were used in this study. $2{,}5*10^8$ spores were used to inoculate 250 ml flasks containing 50 ml liquid NMMP medium, supplemented with 0.5% glucose and 0.5% mannitol (Kieser et al. 2000).

RNA sequencing

Mycelium was collected after 17 h of growth by centrifugation at 5,000 rpm for 10 min. RNA was immediately isolated using the Kirby protocol (Kieser et al. 2000). The samples were treated with DNase I to remove any traces of DNA. The purity and integrity of the sample was assessed using a Bio-Rad Gel Doc EZ Imager, while the absence of residual DNA was verified by PCR (Fig. 1S). The RNA samples were sent for sequencing to BaseClear, after which the RNA quality was further assessed using a Bioanalyzer. Ribosomal RNA was subsequently removed with a Ribo-Zero kit (Epicenter) and the remaining RNA used as input for the Illumina TruSeq RNA-seq library preparation. Once fragmented and converted into double strand cDNA, the fragments (about 100-200 bp) were ligated with DNA adapters at both ends and amplified via PCR. The resulting library was then sequenced using an Illumina Sequencer. The FASTQ sequence reads were generated using the Illumina Casava pipeline version 1.8.3. Initial quality assessment was based on data passing the Illumina Chastity filtering. Subsequently, reads containing adapters and/or PhiX control signals were removed using an in-house filtering protocol. The second quality assessment was based on the remaining reads using the FASTQC quality control tool version 0.10.0.

RNA-seq analysis

The RNA-Seq analysis was performed by Baseclear BV (Leiden, The Netherlands). Briefly, the quality of the FASTQ sequences was enhanced by trimming off low-quality bases using the "Trim sequences" option present in CLC Genomics Workbench Version 6.0.4. The quality-filtered sequence reads were used for further analysis with CLC Genomics Workbench. First an alignment against the reference(s) and calculation of the transcript levels was performed using the "RNA-Seq" option. Subsequent comparison of transcript levels between strains and statistical analysis was done with the "Expression analysis" option, calculating so-called RPKM values. These are defined as the Reads Per Kilobase per Million mapped reads (Mortazavi et al. 2008) and seeks to normalize for the difference in number of mapped reads between samples as well as the transcript length. It is given by dividing the total number of exon reads by the number of mapped reads (in Millions) times the exon length (in kilobases).

SUPPLEMENTAL MATERIAL

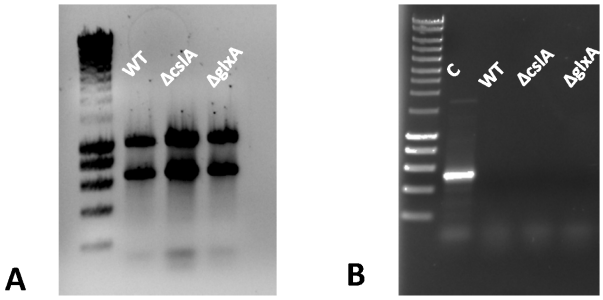

Figure 1S. (A) Quality assessment of the RNA samples on a 1.2% agarose TAE gel. The 23S, 16S and 5S bands are clearly visible in the three samples and no signs of degradation are visible. (B) PCR check for the absence of genomic DNA on 4 µg of RNA as a template. The first lane include a control sample with *S. lividans* genomic DNA.